Optics Letters

Local activation of surface and hybrid acoustic waves in optical microwires

Desmond M. Chow,[1,*] Jean-Charles Beugnot,[2] Adrien Godet,[2] Kien P. Huy,[2] Marcelo A. Soto,[1] and Luc Thévenaz[1]

[1]EPFL Swiss Federal Institute of Technology, Institute of Electrical Engineering, SCI STI LT, Station 11, CH-1015 Lausanne, Switzerland
[2]Institut FEMTO-ST, Université de Franche-Comté, CNRS 15B Avenue des Montboucons, F-25030 Besançon, France
*Corresponding author: desmond.chow@epfl.ch

Received 13 November 2017; accepted 13 February 2018; posted 26 February 2018 (Doc. ID 313347); published 22 March 2018

Elastic vibrations in subwavelength structures have gained importance recently in fundamental light–matter studies and various optoacoustic applications. Existing techniques have revealed the presence of distinct acoustic resonances inside silica microwires yet remain unable to individually localize them. Here, we locally activate distinct classes of acoustic resonances inside a tapered fiber using a phase-correlation distributed Brillouin method. Experimental results verify the presence of surface and hybrid acoustic waves at distinct fiber locations and demonstrate, to the best of our knowledge, the first distributed surface acoustic wave measurement. This technique is important for understanding properties of optoacoustic interactions and enabling designs of novel optomechanical devices.

OCIS codes: (060.2270) Fiber characterization; (290.5900) Scattering, stimulated Brillouin; (130.3990) Micro-optical devices.

https://doi.org/10.1364/OL.43.001487

The rich dynamics of photon–phonon interactions in sub-wavelength dimension structures have generated immense scientific interest lately. Brillouin scattering self-cancellation [1] and surface Brillouin scattering [2] are among the newly discovered optoacoustic interactions in sub-wavelength silica microwires. Surface Brillouin scattering can be described as an inelastic light scattering generated by a surface acoustic wave (SAW) induced via electrostriction. Traveling at the boundary interface of dissimilar elastic stiffness regions, SAWs demonstrate clear advantages over bulk waves for their low speed and accessibility, permitting a wide range of applications, including surface studies, signal processing, time delay, etc. [3]. Unlike the simplified plane wave description of stimulated Brillouin scattering (SBS) in conventional optical fibers, the low dimension and hard mechanical boundary conditions of silica microwires confine elastic waves into eigenmodes. This feature gives rise to a variety of acoustic vibrations featuring different spatial distributions and speeds, among them hybrid shear-longitudinal acoustic waves (HAWs) and SAWs [2]. Being compatible with standard optical fiber, silica microwires simplify the explorations and manipulations of acoustic waves in an isolated mesoscopic phononics structure [4].

The existence of multiple auxiliary elastic resonances in silica microwires has been experimentally verified by detecting the spontaneous Brillouin backscattering generated by thermally excited acoustic waves [2]. Although such measurements merely indicate the existence of multiple elastic resonances in the entire sample, applied techniques so far cannot resolve the exact longitudinal location of each resonance mode inside a microwire. Indeed, the existence of each acoustic mode highly depends on the local diameter of the microwire, and therefore different resonance frequencies are expected to be found at different positions of the tapered fiber section (e.g., in the transition region and waist). Here, we propose a method to stimulate and probe different classes of acoustic waves at specific locations inside an optical microwire, thus pinpointing precisely their respective locations and amplitude. We demonstrate that, by using a correlation-based distributed Brillouin technique [5–7], each Brillouin resonance frequency (mode) can be locally generated at any position over the tapered optical fiber with a spatial resolution of a few centimeters (or even millimeter scale). The technique employed here is based on the use of pump and probe light beams being phase-modulated with a given (same) phase pattern, so that an identical optical phase crossing will occur only at a specific microwire location (defining a so-called correlation peak). At the correlation peak, the locally generated acoustic waves (independently for each acoustic mode) have enough time to be efficiently activated, thus scattering pump light at the corresponding Brillouin resonant frequency [6,7]. This way, the phase-modulated Brillouin interaction technique can be used to simultaneously generate and measure different acoustic waves, including SAWs, with precise location mapping inside microwires. Experimental results are validated, comparing them with numerical results obtained by solving the elastodynamic equation [8,9]. The experimental approach here proposed, combined with the theoretical analysis presented, can open up a previously unexplored way to better understand the physical behaviors of guided acoustic waves with changing structural dimensions. Furthermore, the possibility to activate a well-localized and particular acoustic mode can potentially lead to new kinds of applications, which can

include distributed SAWs sensors, acoustic flying-spot memories, GHz-region Brillouin filters, and avoided crossing quantum gates.

When an intense light from a coherent laser source is launched into an optical fiber, both longitudinal and transverse propagating acoustic waves are electrostrictively stimulated, leading to the well-known SBS [10] and guided acoustic wave Brillouin scattering (GAWBS) [11], which had been used to sense liquids surrounding an optical fiber [12]. In the conventional SBS process, a slow-travelling longitudinal acoustic wave Bragg scatters the incoming light subjected to a Doppler-shifted frequency, satisfying the phase matching conditions between the interacting light waves and acoustic wave, $\nu_B = 2n_{\text{eff}}V/\lambda$, with n_{eff} the effective refractive index of the propagating light, V the acoustic phase velocity, and λ the optical wavelength in vacuum. In standard optical fibers, the short wavelength approximation applies well to the longitudinal acoustic waves as the fiber core is large and the transverse strains could be conveniently neglected [8,9]. However, as the dimension of an optical fiber approaches the acoustic wavelength, the mismatch in the elastic properties between the silica microwire and air results in hard mechanical boundary conditions, causing longitudinal and shear components of acoustic waves to intersect. Thus the acoustic mode branches into several HAWs with different spatial distributions and propagation speeds [2]. Conversely, SAWs originate from the coupling of shear and longitudinal components in an elliptically polarized particle motion along the boundary of two different materials. SAW generation is efficient due to the large evanescent field extending across the mechanical stress-free boundary, shaking the microwire surface to form minuscule moving periodic corrugations, which propagate slower than the bulk transverse wave.

Harnessing the fascinating optoacoustic properties of microwires would be hard without a low-loss transition between the microwire and standard optical fiber. Here we fabricate the microwire by adiabatically tapering a single-mode fiber (SMF) to micrometer scale using a flame brushing technique. An uncoated stretch of standard SMF is heated in a moving flame and pulled apart slowly by a pair of precision translation stages. The fabricated microwire has a taper transition length of ~10 cm, a tapered waist of ~4 cm, and a diameter of ~0.9 μm. The profile of the tapered fiber is a higher order reciprocal function given by a controlled linear hot-zone length variation [13], as shown in Fig. 1, where the position 0 cm corresponds to the center location of the waist. The optical guidance through the microwire is monitored during fabrication to verify the adiabatic optical mode

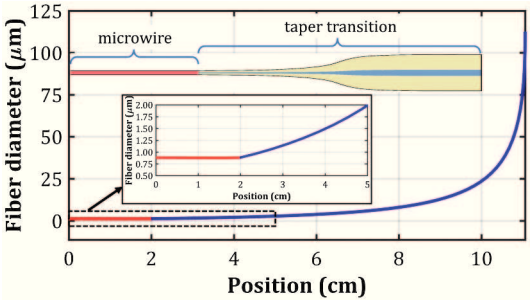

Fig. 1. Taper profile including microwire (red) and transition (blue) regions.

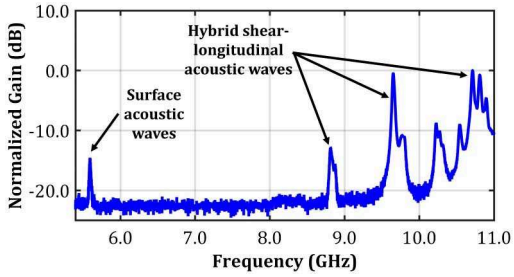

Fig. 2. Integrated stimulated Brillouin scattering gain spectrum measured using counter propagating pump and probe lights. Different acoustic modes are observed as a result of the diameter variation along the tapered optical fiber.

condition. Single-mode guidance is ensured by observing the state of transmitted power and the experimental modal beating.

The presence of distinct elastic waves in the fabricated microwire is verified by launching a counter propagating continuous wave (CW) pump and probe light into the microwire. The probe signal gain is measured as the frequency difference between pump and probe lights is varied from 5.4 GHz to 11 GHz. Figure 2 shows the acquired stimulated Brillouin gain spectrum of the microwire. SAW, due to its distinct resonance frequency, is clearly identified; nevertheless, the classes of different acoustic resonances from 8.8 GHz to 11 GHz are indistinguishable without resolving to their respective location in the microwire.

Phase-correlation-based distributed Brillouin method [6,7] is used to activate and detect different acoustic modes at specific locations along the silica microwire. Figure 3 shows the experimental setup for measuring the local Brillouin gain along the microwire, using counter propagating pump and probe waves. The incoming light from a laser diode (1552 nm) is first phase-modulated by a 1023-bit Pseudo Random Binary Sequence (PRBS) at ~2 GHz clock frequency. The phase-modulated light is then split by a 90/10 coupler into pump and probe arms. Light in the probe arm is intensity-modulated to generate sidebands with a suppressed carrier and passed through a 2 km SMF delay line, which is necessary to place a high-order correlation peak inside the microwire and thus to provide a precise longitudinal sampling interval (increment between the positioning of two consecutive correlation peaks). The Brillouin frequency scanning step is 1 MHz. In the pump arm,

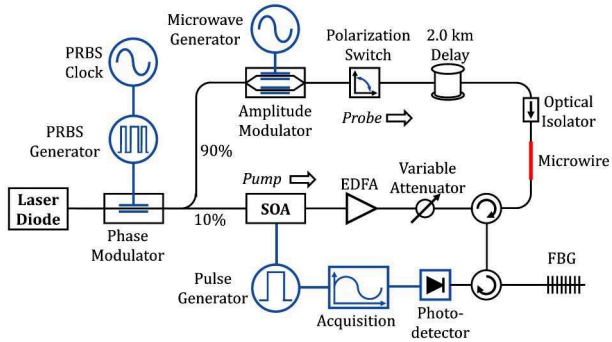

Fig. 3. Experimental setup used for correlation-based distributed Brillouin measurements.

the phase-modulated light is time-gated (intensity-modulated) by a semiconductor optical amplifier (SOA) using pulses of 70 ns with 25 μs repetition period and then amplified by an Erbium-doped fiber amplifier (EDFA). After the pump and probe interact inside the sample, the probe is directed into a detection system, where one of the sidebands is selected by a fiber Bragg grating (FBG) ($\Delta\nu = 6$ GHz) and detected by a photo receiver ($\Delta\nu = 125$ MHz). The detailed operating principles of phase-correlation distributed Brillouin scanning method can be found in [6,7]. The spatial resolution is optimized to give sufficient detected Brillouin gain with a reasonable number of resolved points. The PRBS clock period T determines the correlation peak's full width at half-maximum (FWHM), $\Delta z = 0.5 v_g T$, where v_g is the group velocity of light. FWHM of the correlation peak is evaluated to be ~5.2 cm, assuming an effective refractive index n_{eff} of 1.44 for silica glass. The longitudinal sampling interval is set to 2.5 cm. The spatial resolution depends on both the correlation peak size and the sampling interval [7]. So with the preset oversampling, the spatial resolution can be as small as 60% of the correlation peak FWHM, giving an effective spatial resolution of 3.2 cm. The longitudinal scan is then conducted over 40 cm in total length, covering the waist, transition, and untapered fiber sections.

The spatio-spectral domain of the microwire is scanned by independently sweeping the pump-probe frequency offset and varying slightly the PRBS clock. Note that small changes in the PRBS clock allow for a full longitudinal scan of the entire tapered fiber, having practically a negligible impact on the spatial resolution due to the use of a high-order correlation peak [6,7]. The Brillouin gain spectra (and respective resonance frequencies) are experimentally obtained along the microwire by scanning a frequency range from 5.5 to 11.5 GHz, as shown in Fig. 4. The distance scale in the figure originates in the middle of the waist and increases towards the untapered regions. The Brillouin frequency shift of the untapered standard fiber segments is around 10.815 GHz, as shown in Fig. 4(e) at positions larger than ±12 cm. Results indicate that four acoustic resonances can be clearly identified in the waist (microwire), i.e., around 0 cm: at 5.6 GHz [Fig. 4(a)], 8.8 GHz [Fig. 4(b)], 9.65 GHz [Fig. 4(c)], and 11.45 GHz [Fig. 4(f)]. From these, the resonance at 9.65 GHz gives the highest gain [see the high contrast in Fig. 4(c)], followed by 11.45 GHz and 8.8 GHz. In the transition region (distance from 2 cm to 8 cm), a number of resonance pairs are found at 10.25 GHz, 10.55 GHz, 10.7 GHz, and 10.815 GHz [see Figs. 4(d) and 4(e)], indicating the symmetry of the tapered fiber sample and confirming the structural nature of the acoustic resonances. In the far transition region (distance from 8 cm to 12 cm, i.e., when the taper diameter approaches the standard fiber diameter), an unusual broad scattering band appears from 10.85 to 11.2 GHz [Fig. 4(e)] due to the changes of longitudinal and shear acoustic velocities as the fiber diameter varies, as confirmed by the simulation (see Fig. 5). This band had also been observed using the heterodyne detection technique [1]. The discontinuity between the band and the resonant frequency of the standard optical fiber segment (at 10.815 GHz) can be explained by the rapid diameter reduction and core disappearance in the transition region: as fiber tapers down exponentially to micrometer scale, the Ge-doped core defuses rapidly, forcing the light to propagate in the pure silica cladding and causing the sudden jump in the Brillouin frequency shift.

SAW is the slowest propagating acoustic wave in the microwire, thus leading to the lowest resonant frequency, being of ~5.6 GHz [Fig. 4(a)]. Note that due to the strong pump reflection induced by the taper profile and the close spectral proximity between SAW and pump frequencies, the measurement of SAW has been performed with an enlarged spatial

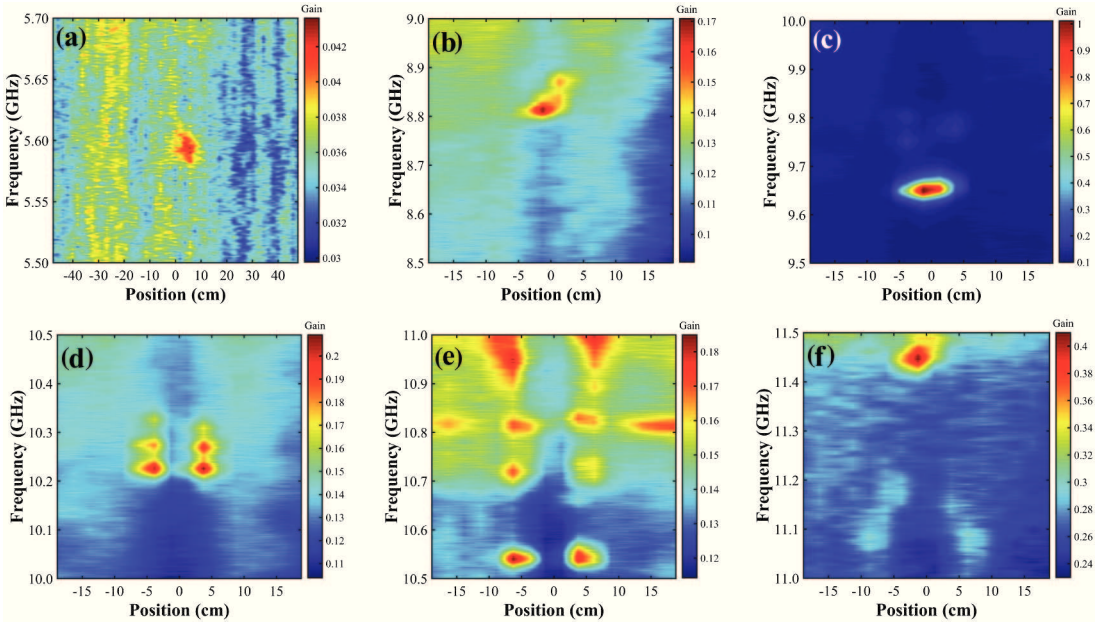

Fig. 4. Phase-correlated distributed Brillouin gain spectra along the silica microwire for frequency ranges (a) 5.5–5.7 GHz, (b) 8.5–9.0 GHz, (c) 9.5–10.0 GHz, (d) 10.0–10.5 GHz, (e) 10.5–11.0 GHz, and (f) 11.0–11.5 GHz. Position 0 cm is the center of the tapered waist. Gain scales are linear, calculated with respect to the detected off-resonance signal level in each scanning region. Note that the horizontal scale of (a) is made narrower to visualize the entire scanning result that has larger spatial resolution.

resolution (~85% longer). Indeed, since the pump and probe spectra broaden with higher spatial resolution (i.e., with large PRBS clock frequencies), sharper spatial resolutions typically lead to overlapping of the phase-modulated pump and probe spectra. This induces real practical challenges in the optical filtering required in reception, especially for the low SAW resonance frequency of 5.6 GHz. To minimize this spectral overlapping, and reduce distortions in the measurements, the PRBS clock frequency for SAW measurement has been reduced down to 1.0 GHz, resulting in a correlation peak FWHM of 10 cm. With oversampling, the spatial resolution could be improved down to about 6 cm, covering the uniform microwire region in a single sampled point. Note that the measurements in Fig. 4(a) indicate that the phase-correlation Brillouin method used in this case allows for distributed measurements of Brillouin SAW, representing, to our best knowledge, the first demonstration of distributed SAW measurements.

The experimental results are subsequently confirmed through numerical modeling using the elastodynamic equation describing the propagation of acoustic waves including the contribution of electrostriction [8,9]:

$$\rho\frac{\partial^2 u}{\partial t^2}-\frac{\partial}{\partial x_j}\left(c_{ijkl}\frac{\partial u_k}{\partial x_l}\right)=\frac{\partial}{\partial x_j}\epsilon_0\chi_{klij}E_kE_l^*.$$

The left-hand side describes the acoustic waves, where u_i are the element displacements, ρ is the material density, and c_{ijkl} is the rank-4 elastic tensor; the right-hand side term gives the electrostrictive volume force, where E_k and E_l are the pump and Brillouin Stokes fields, and the rank-4 susceptibility tensor is $\chi_{klij}=\epsilon_{im}\epsilon_{jn}p_{klmn}$ with p_{klmn} being the elasto-optic tensor. ϵ_0 is the permittivity of vacuum. Using a finite element method, the equation is applied on the microwire cross section and solved for the backward propagating case, obtaining the total elastic energy that includes all longitudinal and transversal displacement components.

As shown in Fig. 5, the spectrum of elastic energy density is retrieved by varying the wire diameter according to the tapering profile. As indicated in labels (a), (b), (c), and (f), all the acoustic resonant frequencies at the taper waist (microwire) agree with the measurements, except the resonances at 7.0 GHz and 10.4 GHz due to the weak gain. Nevertheless, all of them are about 0.3 GHz higher than the numerical model, which could be due to the slight change in strain during microwire packaging, temperature variation, or slight departure from the intended microwire diameter during fabrication. In the transition region, acoustic resonance branching appears at shear and longitudinal wave intersections that form multiple avoided crossings. Since the Brillouin gain is spatially integrated over the correlation peak width in the experiment, the tails extending out from most resonant peaks are not clearly visible with the exception of the fleeting extensions for resonances at 8.8 GHz [Fig. 4(b)] and 9.65 GHz [Fig. 4(c)]. Higher up in the tapered fiber dimension, acoustic mode splitting is vague, yet the superposition of the adjoining resonances gives rise to a broad scattering band [label (e)] as noticed in the experiment [Fig. 4(e)], which expands gradually as the taper diameter approaching the micrometer scale.

In conclusion, in this Letter we have demonstrated the generation and detection of localized SAWs and different classes of hybrid acoustic waves along a microwire using a phase-correlation-based distributed Brillouin interrogation method. Experimental results reveal the diverse acoustic spatio-spectral dynamics inside a microscale structurally varied optical waveguide, presenting a convenient way to study the physics of local SAWs, HAWs, shear wave propagation, coupling regimes at avoided crossing, etc. The study reveals the interest of an intermediate region where the fiber diameter is in the range 5–10 μm, for which the acoustic resonances vary stepwise and not continuously. The successful demonstration of SAW-distributed Brillouin mapping opens a way to realize distributed optomechanical sensors in optical fibers. In general, this technique also provides huge potential for acoustic engineering in subwavelength waveguides given the ability to access acoustic properties at arbitrary points, thus effectively turning a continuous optical fiber into a multi-element acoustic device or sensor. Further developments aim at understanding the interactions between different acoustic waves and the surrounding environment.

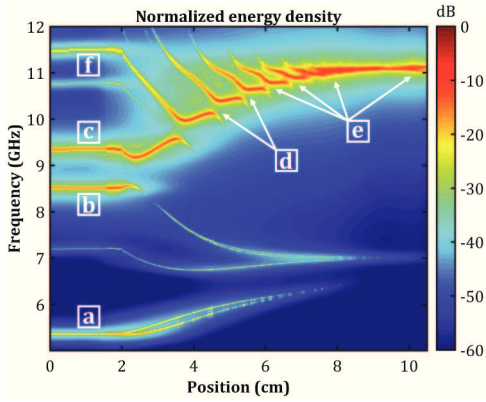

Fig. 5. Numerical simulations of elastic energy density (the results are adapted from [2,14]). Labels (a)–(f) indicate the corresponding acoustic modes measured in Figs. 4(a)–4(f).

Funding. Swiss National Science Foundation (SNF) (200021L-157132).

REFERENCES

1. O. Florez, P. F. Jarschel, Y. A. Espinel, C. Cordeiro, T. M. Alegre, G. S. Wiederhecker, and P. Dainese, Nat. Commun. **7**, 11759 (2016).
2. J.-C. Beugnot, S. Lebrun, G. Pauliat, H. Maillotte, V. Laude, and T. Sylvestre, Nat. Commun. **5**, 5242 (2014).
3. R. M. White, Proc. IEEE **58**, 1238 (1970).
4. A. A. Balandin and D. L. Nika, Mater. Today **15**(6), 266 (2012).
5. K. Hotate and T. Hasegawa, IEICE Trans. Electron. **83**, 405 (2000).
6. A. Zadok, Y. Antman, N. Primerov, A. Denisov, J. Sancho, and L. Thevenaz, Laser Photon. Rev. **6**, L1 (2012).
7. A. Denisov, M. A. Soto, and L. Thévenaz, Light Sci. Appl. **5**, e16074 (2016).
8. V. Laude and J.-C. Beugnot, AIP Adv. **3**, 042109 (2013).
9. J.-C. Beugnot and V. Laude, Phys. Rev. B **86**, 224304 (2012).
10. E. Ippen and R. Stolen, Appl. Phys. Lett. **21**, 539 (1972).
11. R. Shelby, M. Levenson, and P. Bayer, Phys. Rev. B **31**, 5244 (1985).
12. Y. Antman, A. Clain, Y. London, and A. Zadok, Optica **3**, 510 (2016).
13. T. A. Birks and Y. W. Li, J. Lightwave Technol. **10**, 432 (1992).
14. A. Godet, A. Ndao, T. Sylvestre, V. Pecheur, S. Lebrun, G. Pauliat, J.-C. Beugnot, and K. P. Huy, Optica **4**, 1232 (2017).